

ATraDiff: Accelerating Online Reinforcement Learning with Imaginary Trajectories

Qianlan Yang¹ Yu-Xiong Wang¹

Abstract

Training autonomous agents with sparse rewards is a long-standing problem in online reinforcement learning (RL), due to low data efficiency. Prior work overcomes this challenge by extracting useful knowledge from offline data, often accomplished through the learning of action distribution from offline data and utilizing the learned distribution to facilitate online RL. However, since the offline data are given and fixed, the extracted knowledge is inherently limited, making it difficult to generalize to new tasks. We propose a novel approach that leverages offline data to learn a generative diffusion model, coined as *Adaptive Trajectory Diffuser (ATraDiff)*. This model generates synthetic trajectories, serving as a form of data augmentation and consequently enhancing the performance of online RL methods. The key strength of our diffuser lies in its adaptability, allowing it to effectively handle varying trajectory lengths and mitigate distribution shifts between online and offline data. Because of its simplicity, ATraDiff *seamlessly integrates with a wide spectrum of RL methods*. Empirical evaluation shows that ATraDiff consistently achieves state-of-the-art performance across a variety of environments, with particularly pronounced improvements in complicated settings. Our code and demo video are available at <https://atradiff.github.io>.

1. Introduction

Deep reinforcement learning (RL) has shown great promise in various applications, such as autonomous driving (Wang et al., 2019), chip design (Mirhoseini et al., 2021), and

¹Department of Computer Science, University of Illinois Urbana-Champaign, Urbana, Illinois, USA. Correspondence to: Qianlan Yang <qianlan2@illinois.edu>.

Proceedings of the 41st International Conference on Machine Learning, Vienna, Austria. PMLR 235, 2024. Copyright 2024 by the author(s).

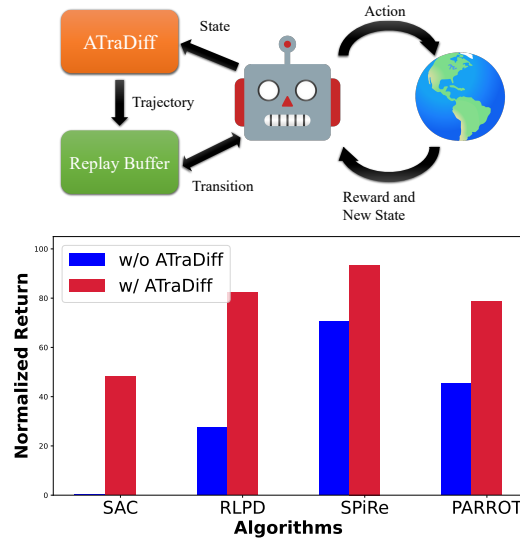


Figure 1. Illustration and performance showcase of our ATraDiff. ATraDiff can seamlessly integrate with a wide range of RL methods and consistently improve their performance, by augmenting the replay buffer with synthesized trajectories. **Top:** Overview of online RL with ATraDiff. **Bottom:** Performance comparison of RL methods with and without ATraDiff in D4RL Kitchen.

energy optimization (Specht & Madlener, 2023). Despite its impressive performance, RL often requires extensive online interactions with the environment, which can be prohibitively costly in practice. Such downside of RL is aggravated by the fact that in real-world scenarios, environments are often characterized by sparse rewards, which further necessitates an exceptionally large number of samples for effective exploration. For example, when manipulating a robotic arm to move an item, oftentimes the only reward feedback given is at the success moment of the task, which may take hundreds of steps to obtain. Consequently, a persistent challenge in RL is addressing the high sample costs, particularly in contexts with sparse rewards.

One prevalent solution to this challenge is leveraging offline data, by directly learning policies from offline data (Kostrikov et al., 2022; Ball et al., 2023) or extracting experiences that can enhance online training (Pertsch et al., 2020), especially in the context of exploration. How-

ever, such solutions can only extract limited knowledge as the offline data are given and fixed, and thus are difficult to generalize to new tasks. In contrast to prior work, this paper takes a different perspective inspired by the recent advances in generative modeling – *can we harness modern generative models, such as diffusion models, trained on offline data and synthesize useful data that facilitate online RL?*

Indeed, diffusion models have emerged as powerful deep generative models, demonstrating impressive capabilities in data synthesis across vision and language applications (Ho et al., 2020; Gong et al., 2023; Li et al., 2022). Nevertheless, their investigation in RL has been relatively limited. Studies in offline RL mainly tap into the generative capabilities of diffusion models to enhance long-term planning (Janner et al., 2022; Ajay et al., 2023) and amplify policy expressiveness (Wang et al., 2023; Chen et al., 2023). Recently, SynThER (Lu et al., 2023) is introduced to utilize diffusion models for RL data augmentation, by upsampling the data with a diffusion model trained on an offline dataset. However, such an approach primarily focuses on generating *transitions* rather than *complete trajectories*. This under-utilizes the generative potential of diffusion models and limits the benefits of augmented data for RL. In contrast, full trajectories offer a more comprehensive source of information, enabling RL agents to better learn from past experiences.

To overcome these issues, we propose *Adaptive Trajectory Diffuser (AtraDiff)*, a novel method designed to synthesize full trajectories for online RL. As depicted in Figure 1, our approach trains a diffusion model using offline data, which then synthesizes complete trajectories conditioned on the current state. By employing this diffusion model to produce additional trajectories, we aim to significantly accelerate the online RL process. Notably, because of its simplicity in augmenting the replay buffer by adding useful data, AtraDiff *seamlessly integrates with a wide range of RL methods* and *consistently elevates their performance*.

The key property of our diffuser lies in its *adaptability* to effectively handle varying trajectory lengths and address the distribution shifts between online and offline data. Unlike generating transitions, managing the uncertainty in task lengths presents a significant new challenge in trajectory generation. While longer trajectories can potentially lead to improved performance, excessive or redundant segments may be detrimental. Ideally, we aim for a generation with a precise trajectory length. To this end, we introduce a simple yet effective *coarse-to-precise* strategy: initially, we train multiple diffusion models with varying generation lengths. Prior to actual generation, we assess the required length and subsequently prune any redundant segments. In dealing with the distribution shift between offline data and online evaluation tasks, we design our diffuser to be adaptable throughout the RL process. This adaptability includes the capability

to select more informative samples through the use of an *importance indicator*, while also mitigating catastrophic forgetting during adaptation.

Our contributions are three-fold. (i) We propose AtraDiff, a novel diffusion-based approach that leverages offline data to generate full synthetic trajectories and enhance the performance of online RL methods. AtraDiff is general and can be seamlessly applied to accelerate *any* online RL algorithm with a replay buffer, as well as being effective in offline environments. (ii) We introduce a simple yet effective coarse-to-precise strategy that ensures generated trajectories precisely align with the length required for evaluation tasks. (iii) We devise an online adaptation mechanism that successfully addresses challenges stemming from data distribution shifts. Empirical evaluation shows that AtraDiff consistently achieves state-of-the-art performance across a variety of *online, offline-to-online, and offline* environments, with particularly large improvements in complicated settings.

2. Related work

Offline pretraining for online RL. Leveraging prior experiences to expedite online learning for subsequent tasks has been a persistent challenge (Nair et al., 2021). Past research has proposed numerous solutions to tackle this issue. Some studies suggest treating offline data similarly to data collected online. Representative approaches employ offline data to initialize a replay buffer (Večerík et al., 2017; Hester et al., 2018). Meanwhile, others advocate for a balanced sampling strategy, drawing from both offline and online sources (Nair et al., 2018; Kalashnikov et al., 2018; Hansen et al., 2023; Zhang et al., 2023; Ball et al., 2023).

One prevalent strategy is to establish a behavior prior, which captures the action distribution in prior experiences to mitigate overestimation for actions outside the training data distribution (Singh et al., 2021; Siegel et al., 2020). An alternative strategy involves extracting skills from offline data and adapting them to new tasks (Gupta et al., 2019; Merel et al., 2019; Kipf et al., 2019; Whitney et al., 2020; Pertsch et al., 2020). These studies typically represent the acquired skills within an embedding space and then train a policy to select the most appropriate skills based on the current state. In contrast, AtraDiff synthesizes the complete trajectory based on the current state and augments the replay buffer with these additional data. Our approach offers broader applicability across a diverse set of RL methodologies.

Diffusion models in RL. The focus of employing diffusion models in RL has primarily centered on enhancing long-term planning and amplifying policy expressiveness. For instance, Diffuser (Janner et al., 2022) constructs a full trajectory of transitions, through conditioned sampling guided by higher rewards and goal-oriented navigation. This lever-

ages the diffusion model’s capability in generating extensive trajectories, addressing challenges such as long horizons and sparse rewards in RL planning. Other studies (Ajay et al., 2023; Du et al., 2023; He et al., 2023) have adopted this paradigm, particularly in the context of visual data. Another notable work (Pearce et al., 2023) suggests a diffusion-based method for generating full trajectories by imitating human behavior. Different from prior work, our approach is oriented towards synthesizing trajectories in evaluation scenarios that may differ from the training scenarios.

Data augmentation in RL. Data augmentation is a common technique that has demonstrated effectiveness in RL. Previous methods (Yarats et al., 2021; Laskin et al., 2020; Sinha et al., 2021) typically focus on perturbing original observation data in visual-based RL, such as adding noise and applying random translation. This enables agents to learn from multiple views of the same observation and increase their robustness. Recent efforts have focused on upsampling the replay buffer with the diffusion model. A closely related study, SynthER (Lu et al., 2023), generates transitions to augment the replay buffer via a diffusion model. However, our AtraDiff *operates at the trajectory level, can employ a visual-based diffusion model, and has the capability to synthesize training data through state- and task-conditioned generation.* Furthermore, our work primarily focuses on leveraging offline data to enhance online RL performance. In contrast, SynthER aims to upsample the offline dataset using its data synthesizer. Our setting thus presents more complex challenges, involving dynamic generation and managing the distribution shift between offline and online data. Another work (He et al., 2023) investigates training a diffusion model to enhance multi-task learning, whereas we develop a general method to improve any RL method.

3. Background

MDP. In this paper, we consider sequential decision-making tasks that can be modeled as a Markov Decision Process (MDP) defined as $\mathcal{M} = \langle S, A, T, R, \gamma \rangle$, where S is the set of states, A is the set of actions, and $\gamma \in [0, 1)$ is the discount factor. $T(s'|s, a)$ and $R(s, a)$ represent the dynamics and reward functions, respectively. At each stage t , the agent takes an action $a \in A$, which leads to a next state s' according to the transition function $T(s'|s, a)$ and an immediate reward $R(s, a)$. A trajectory of such a task is defined as a sequence composed of states and actions given by $(s_1, a_1, s_2, a_2, \dots, s_t, a_t)$, where s_t and a_t denote the state and action at time-step t , respectively.

Diffusion models. Diffusion probabilistic models pose the data-generating process as an iterative denoising procedure $p_\theta(\tau^{i-1}|\tau^i)$. This denoising is the reverse of a forward diffusion process $q(\tau^i|\tau^{i-1})$ that slowly corrupts the structure in data by adding noise in N steps, where τ^i is the i -step of

the denoising process. The data distribution induced by the model is given by:

$$p_\theta(\tau^0) = \int p(\tau^N) \prod_{i=1}^N p_\theta(\tau^{i-1}|\tau^i) d\tau^{1:N},$$

where $p(\tau^N)$ is a standard Gaussian prior and $p(\tau^0)$ denotes noiseless data. Parameters θ are optimized by minimizing a variational bound on the negative log-likelihood of the reverse process: $\theta^* = \arg \min_\theta -\mathbb{E}_{\tau^0} [\log p_\theta(\tau^0)]$. The reverse process is often parameterized as Gaussian with fixed timestep-dependent covariances:

$$p_\theta(\tau^{i-1}|\tau^i) = \mathcal{N}(\tau^{i-1}|\mu_\theta(\tau^i, i), \Sigma^i).$$

Replay buffers. Many algorithms in RL employ replay buffers, denoted as D , to retain trajectories derived from executing a sample policy within an environment parameterized by MDP. Throughout the training process, these replay buffers are accessed to extract samples (transitions or trajectories) for updating the learned execution policy.

4. Method

We now present our approach to accelerating online reinforcement learning by training our generative model AtraDiff on the offline data to synthesize trajectories. We begin by introducing how we design and train AtraDiff (Section 4.1) and then explain how we apply AtraDiff to accelerate online reinforcement learning (Section 4.2). Finally, we introduce how this generator could be dynamically adapted during the online training process (Section 4.3). Figure 2 illustrates the overall framework of our approach.

4.1. Adaptive Trajectory Diffuser

Our primary objective with the generator is to train a diffusion model $p(\cdot)$ that captures the trajectory data distribution present within the offline data. By doing so, we can synthesize new trajectories $(s_1, a_1, r_1, s_2, a_2, r_2, \dots, s_t, a_t, r_t)$ with the learned diffusion model. Our work introduces a general data generation framework that is *agnostic* to the specific form of generation: we investigate both *state-level* and *image-level* generation. The state-level generation is to directly generate the states, actions, and rewards from the diffusion model which is trained from scratch. In contrast, image-level generation allows us to benefit from powerful pretrained models, which potentially leads to improved performance. To harness these models more effectively, we advocate for the synthesis of trajectory *images* rather than direct generation of states. Specifically, our strategy entails initially generating images $I_1, I_2, I_3, \dots, I_k$ spanning k continuous frames, where k is a fixed generation length preset for a given generator. Subsequently, we can get the state, action, and reward s_i, a_i, r_i from the resultant images

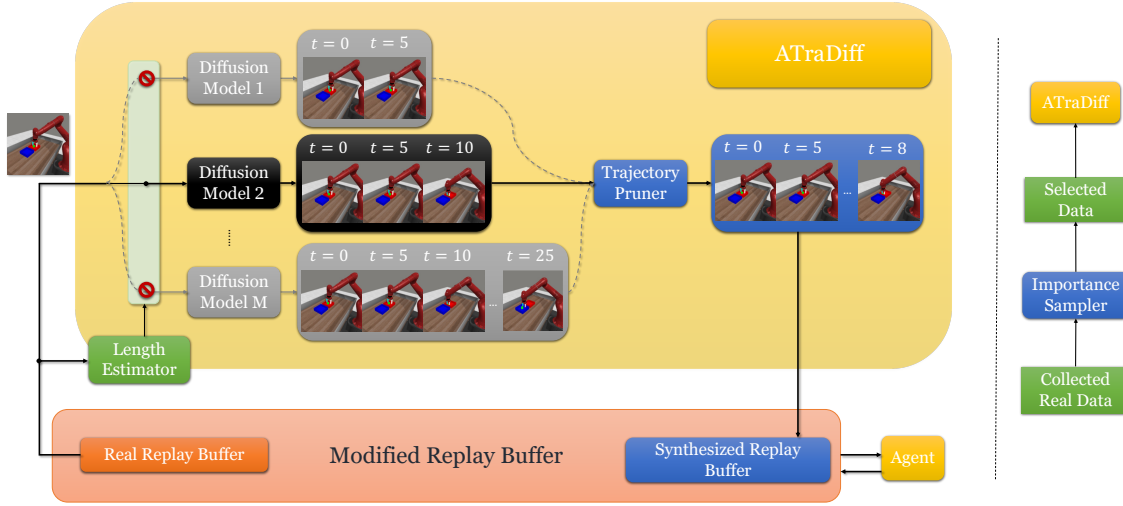


Figure 2. Illustrative overview of our ATraDiff framework. **Left:** A diffuser containing multiple diffusion models, a length estimator, and a trajectory pruner. **Right:** Workflow of the online adaptation.

using a trained *decoder* that converts images into states. Conversely, to provide images for our generator, we use another *encoder* to convert states into images. We implement the *encoder* by simple ray tracing (Shirley, 2000). More details are provided in Appendix A.

Image diffusion models. For the architecture design of our image diffuser, we use Stable Diffusion (Rombach et al., 2022) as the pretrained model and fine-tune it on the specific dataset. To generate images of k continuous frames, we concatenate the k single images I_1, I_2, \dots, I_k into one larger 2D image \mathcal{I} by aligning them in order and use the diffusion model to generate the concatenated image \mathcal{I} . Furthermore, we use the information of the first frame as the generation condition, including the current state, task, etc., so that the generated trajectory will be closely related to our learning process, where online learning could benefit more from these synthesized data.

End-to-end decoder. We design a decoder to decode states, actions, and rewards from the generated images. The decoder is a neural network consisting of two components. The first component incorporates the feature distilled from the diffusion layer (Zhao et al., 2023). In the second component, separate multilayer perception (MLP) networks are used to determine the 3D positions of specific key points, which are used to generate the real states. This two-component design of the decoder allows for efficient processing of the images, by first identifying relevant features through the diffusion model and then pinpointing key points’ positions using MLP networks, so that we can calculate the proprioceptive states. The rewards and actions are predicted from the features and the predicted states with separate MLP networks.

Generation of Trajectories with Flexible Lengths. Due

to the property of diffusion models, our diffuser described above can only obtain trajectories with a fixed length of k ; however, to generate a complete trajectory where the horizon is indefinite, we would require the diffuser to output trajectories with flexible lengths, which becomes the crucial problem. To solve this, we introduce a simple *coarse-to-precise* strategy. We initially train multiple (M) diffusion models with varying lengths, such as $k = 5, 10, 15, \dots$. Before generation, we first estimate the required length for the current state with a pretrained network and round it up to the nearest preset length, minimizing the occurrence of redundant transitions. To prune the redundant segment after generation, we introduce a *non-parametric* algorithm to identify the best ending position.

More concretely, for a generated trajectory (s_1, s_2, \dots, s_k) , we first calculate the similarity between each of two adjacent states, $\text{sim}(s_1, s_2), \text{sim}(s_2, s_3), \dots, \text{sim}(s_{k-1}, s_k)$. Then we compute the prefix average pre_i and suffix average suf_i of this similarity sequence, where $\text{pre}_i = \frac{\sum_{j=1}^i \text{sim}(s_j, s_{j+1})}{i}$, $\text{suf}_i = \frac{\sum_{j=i}^k \text{sim}(s_{j-1}, s_j)}{k-i+1}$. Then we get the difference between the prefix average and suffix average $|\text{pre}_i - \text{suf}_i|$ of each position i ($1 < i < k$), and find the one with the largest difference to be the ending position.

This trajectory pruning algorithm operates under the assumption that the average similarity before the ending point should be significantly lower than that after the ending point. This is achieved by training the diffusion model in a way that produces nearly duplicated frames within a redundant segment. To this end, we preprocess the training dataset to *explicitly* introduce redundant segments. Specifically, when training the diffusion model with a generation length of k , given a full trajectory (I_1, I_2, \dots, I_t) , we first append k

Algorithm 1 Modified Replay Buffer for RL

Require: $D = (D_s, D_o, \rho, L)$, ATraDiff.

```

1: function Store  $D, z = (s, a', s', r)$ 
2:   ReplayBufferStore( $D_o, z$ )
3:   if with probability  $\frac{\rho}{(1-\rho)L}$  then
4:      $(s_1, a_1, r_1, \dots, s_l, a_l, r_l) \leftarrow \text{ATraDiff}(s')$ 
5:     for  $\forall i$  do
6:        $z_i = (s_i, a_i, s_{i+1}, r_i)$ 
7:       ReplayBufferStore( $D_s, z_i$ )
8:     end for
9:   end if
10: end function
11:
12: function Sample  $D$ 
13:   if with probability  $\rho$  then
14:      $z \leftarrow \text{ReplayBufferSample}(D_s)$ 
15:   else
16:      $z \leftarrow \text{ReplayBufferSample}(D_o)$ 
17:   end if
18:   return  $z$ 
19: end function

```

additional frames identical to the last frame I_t after the end of the trajectory, resulting in $(I_1, I_2, \dots, I_t, I_t, I_t, \dots, I_t)$. Subsequently, we sample t different sub-trajectories from the padded trajectory, each with a length of k , where the starting position of the sub-trajectory ranges from 1 to t . Hence, for the sub-trajectories starting after time-step $t - k$, their final several frames would always be the same.

4.2. Diffuser Deployment

With the diffuser of ATraDiff explained, we now delve into how the diffuser can be seamlessly integrated with any online RL method with a replay buffer. Intuitively, ATraDiff augments the replay buffer with the data synthesized by its diffuser, and leaves the RL algorithm itself untouched; thus, our approach is orthogonal to any online RL method equipped with a replay buffer.

More specifically, consider any RL algorithm with a replay buffer denoted as D_o . Typically, RL methods engage with the replay buffer through two primary actions: *store*, which archives a new transition into the replay buffer, and *sample*, which extracts a transition randomly from the replay buffer. With this in mind, we substitute the original buffer D_o with a new replay buffer $D = D_o \cup D_s$, where D_s is the augmenting buffer synthesized by ATraDiff. This modified replay buffer D is characterized by two hyperparameters: $\rho \in [0, 1]$, denoting the probability of sampling from synthesized data D_s in RL, and $L \in \mathbb{N}$, indicating the expected length of synthesized trajectories.

Whenever we *store* a transition (s, a, s', r) into D during

the RL algorithm, the following three steps are performed:

- We first *store* it into D_o ;
- With probability $\frac{\rho}{(1-\rho)L}$, a full trajectory $(s_1, a_1, r_1, s_2, a_2, r_2, \dots, s_l, a_l, r_l)$ is synthesized with the diffuser, with state s' as the initial state (i.e., $s_1 = s'$). Note the probability $\frac{\rho}{(1-\rho)L}$ is designed to keep the ratio between the total size of D_s and D_o to be $\frac{\rho}{1-\rho}$;
- All synthesized transitions (s_i, a_i, s_{i+1}, r_i) will be *stored* to the replay buffer D_s .

When we *sample* from D , we *sample* from D_s with probability ρ and from D_o with probability $1 - \rho$. See Alg. 1 for pseudo-code. Note that the sampling process can be arbitrary, i.e., our method is also orthogonal to other sampling techniques such as prioritized buffer (Schaul et al., 2016).

In our algorithm, the expected length, denoted as L , and the actual length, denoted as l , serve distinct purposes and are derived through different methods. The expected length L is defined as the mean length of all trajectories generated during the training phase. It is empirically determined by averaging the lengths of all trajectories generated in preliminary empirical experiments, conducted before the actual training phase. As a critical hyperparameter, L guides the total number of transitions generated by ATraDiff, ensuring a controlled and predictable size of the generated dataset. Conversely, the actual length l is determined subsequent to the generation process. Within this phase, the appropriate generator is selected via the length estimator, followed by trajectory pruning to achieve the desired length. The value of l is inherently variable, adjusting across different generation instances to align with the dynamic contexts and specific requirements of each. Over the course of the training phase, we expect that the mean of all actual lengths l to converge towards the predefined expected length L .

4.3. Online Adaptation

Although the fixed ATraDiff can improve the performance of RL methods in some simple environments, we may still face the problem of distribution shift between the evaluation task and the offline data in complicated environments. To overcome this issue and further improve the generation quality, we propose an online adaptation technique by continually training the diffusion model on new experiences.

Concretely, ATraDiff is periodically updated on the real transitions stored in D_o and then used to generate new trajectories. Meanwhile, we keep a copy of the original version of the diffuser to mitigate potential catastrophic forgetting.

Furthermore, we use more valuable samples to adapt our ATraDiff during online training. Specifically, we design an

indicator to measure the importance of each sample for our online learning, and a *pick-up* strategy to choose samples from D_o . By default, we are introducing two indicators: the TD-error indicator, and the Reward indicator. For the TD-error indicator, the importance of a transition (s, a, s', r) is defined to be $|r + \gamma \max_{a'} Q(s', a') - Q(s, a)|$, where Q is the learned value function. The TD-error indicator performs better in most cases, despite that it could only be used in some value-based RL methods. The Reward indicator would be more general to all RL methods, as the importance of a transition is defined to be the total reward collected in the full trajectory. The primary pick-up strategy is to maintain a subset of samples with higher importance, but part of the samples are always used to update the diffuser. Hence, we randomly drop some samples from the maintained subset regardless of their importance. We further conduct experiments to analyze the effectiveness of our indicator and pick-up strategy and the impact of different design choices in the ablation study.

5. Experiments

We conduct comprehensive experiments to evaluate the effectiveness of our data generator ATraDiff. First, we validate that our approach is able to improve the performance of both basic and state-of-the-art online RL methods by combining them with our ATraDiff (Section 5.1). Next, we show that our method can further improve the performance of a variety of state-of-the-art offline-to-online RL algorithms in complicated environments using online adaptation (Section 5.2). In addition, we evaluate our method in the offline setting to show that ATraDiff achieves promising results in offline data augmentation as well (Section 5.3). Finally, we conduct some ablation studies to validate the effectiveness of different components in our approach (Section 5.4). For evaluation, all results in this section are presented as the median performance over 5 random seeds along with the 25%-75% percentiles.

5.1. ATraDiff Improves Online RL

We first show that the performance of state-of-the-art online RL methods can be improved by our ATraDiff learned with the offline data. We consider 3 environments from D4RL Locomotion (Fu et al., 2020), including 12 different offline data with varying levels of expertise. For comparison, we choose SAC (Haarnoja et al., 2018) as the basic online RL algorithm and REDQ (Chen et al., 2021) as the state-of-the-art sample-efficient algorithm. We run both baselines and their variants combined with our ATraDiff for 250K steps.

The overall result is summarized in Figure 3, showcasing the average performance of each environment with 4 different offline datasets. Detailed performance breakdowns are provided in Appendix C.1. We see that the performance

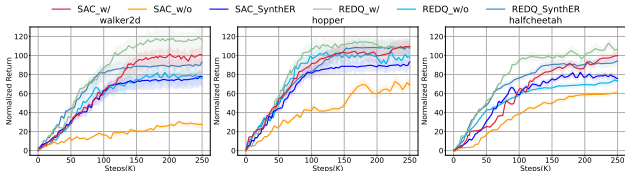


Figure 3. Learning curves of online RL on the D4RL Locomotion benchmark. ATraDiff (denoted as ‘w/’) consistently and significantly improves the performance of the two representative RL methods across all three environments, irrespective of whether basic or advanced algorithms are employed. ATraDiff also outperforms SynthER which synthesizes transitions. These results validate the effectiveness and generalizability of our diffuser.

of the two baselines is both significantly improved by our ATraDiff, especially on the halfcheetah and walker2d environments. This validates the strength of ATraDiff. If we run these online RL methods for enough time, they can also achieve comparable results, while ATraDiff improves the sample efficiency. Here, we only utilize the fixed diffuser instead of using online adaptation, which indicates that our fixed diffuser can already accelerate online RL in some simple environments.

5.2. ATraDiff Improves Offline-to-Online RL in Complicated Environments

In this section, we show that ATraDiff with online adaptation can improve the performance of the state-of-the-art offline-to-online RL methods. We further consider the following environments:

D4RL AntMaze (Fu et al., 2020). There are 6 sparse reward tasks that require the agent to learn to walk with controlling an 8-DoF Ant robot and navigate through a maze to reach the goal.

D4RL Kitchen (Fu et al., 2020). A simulated kitchen environment is proposed by Gupta et al. (2019), which involves controlling a 9-DoF robot that manipulates different objects in a kitchen environment (e.g., slide cabinet door, switch overhead light, and open microwave). The downstream task is to complete a sequence of multiple subtasks in order with a sparse, binary reward for each successfully completed subtask. The offline dataset only contains part of the full sequence, meaning that the agent needs to learn to compose sub-trajectories.

Meta-World (Yu et al., 2019). By combining the modified tasks using a single camera viewpoint consistently over all the 15 subtasks generated by Seo et al. (2022), we create two challenging tasks. The first one is a multi-task setting, where the offline data contain the trajectories of 14 subtasks and 1 different evaluation subtask. The second one is a harder version of the D4RL Kitchen task, where the agent needs to complete a sequence of 8 subtasks with medium difficulty

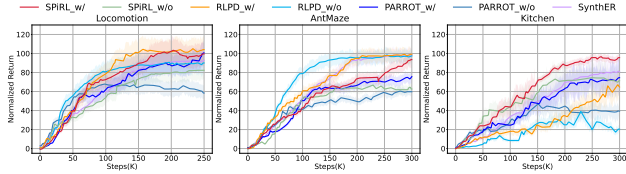


Figure 4. Learning curves of offline-to-online RL on the D4RL benchmark. ATRA diff (denoted as ‘w/’) further boosts the performance of advanced and recent offline-to-online RL baselines across all three environments, leading to state-of-the-art results especially in complex settings, where the improvements are particularly noteworthy. This shows the importance of our online adapted diffuser. The curve named “SynthER” shows the best performance of SynthER combined with any of the baselines.

in the correct order, while the offline data only contain trajectories for single subtasks. The environment will be set to the initial state of the next subtask, when the previous one was completed by the agent. This design ensures that the agent progresses through the tasks in the predetermined order, with objects from different tasks kept isolated to prevent interference. For both tasks, the trajectories of any single subtask consist of the provided data and collected data from the online training.

We consider a set of strong baselines from prior work on offline-to-online RL, including the skill-based method (SPiRL (Pertsch et al., 2020)), behavior-prior-based method PARROT (Kumar et al., 2022), and balanced sampling method RLPD (Ball et al., 2023). We run these baselines and their variants combined with our diffuser. To show the effectiveness of our method, we also compare it with SynthER (Lu et al., 2023). For the following results, the curve named “SynthER” shows the best performance of SynthER combined with any of the baselines.

As shown in Figure 4, our diffuser significantly improves the performance of some methods, and obtains at least comparable results for all methods. For all these environments, the best result is always achieved by some method combined with our diffuser, which shows that our online adapted diffuser can further improve the performance of current offline-to-online methods. Notably, we introduce two advanced tasks within the Meta-World environment to emphasize the challenges posed by distribution shifts. Our motivation is to understand how our method responds under conditions where distribution shift problems are more pronounced. As demonstrated in Figure 5, our approach exhibits superior performance, suggesting that our method holds significant promise in effectively addressing such shifts.

5.3. ATRA Diff Improves Offline RL

Although ATRA diff is primarily intended for offline-to-online scenarios, it also demonstrates strong performance

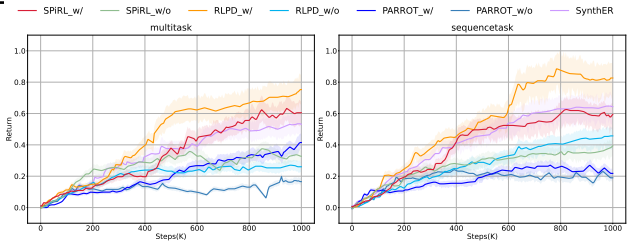


Figure 5. Learning curves of offline-to-online on the Meta-World benchmark. While the two tasks within the Meta-World environment are designed purposefully to be very changing with considerable distribution shifts, ATRA diff (denoted as ‘w/’) is still effective and significantly improves the performance of advanced and recent offline-to-online RL baselines. This further validates the strength of ATRA diff in tackling distribution shifts between offline data and online tasks. The curve named “SynthER” shows the best performance of SynthER combined with any of the baselines.

in offline data augmentation. This section details experiments conducted to assess ATRA diff’s effectiveness in an exclusively offline environment.

Our objective is to verify whether ATRA diff can match or surpass the results achieved in previous research, specifically referencing the work SynthER (Lu et al., 2023) which synthesizes *transitions*. To ensure a fair and accurate comparison, we meticulously replicated the experimental settings used in Lu et al. (2023). We also compare with the previous state-of-the-art augmentation method S4RL (Sinha et al., 2021). Our testing ground is the D4RL Locomotion benchmark (Fu et al., 2020). We extend the original dataset to 5M samples, following the settings in Lu et al. (2023).

The findings, as outlined in Table 1, are quite revealing. They indicate that our ATRA diff method generally outperforms other baselines across various datasets. This performance improvement is particularly pronounced in high-quality datasets, underscoring the effectiveness of our approach in generating helpful trajectories and the benefits of *trajectory-level generation over transition-level generation*.

5.4. Ablation Study and Analysis

In this section, we carry out ablation studies to justify the effect of different components of our ATRA diff. Additional ablation studies are provided in Appendix C.3 and the generated trajectories are visualized in Appendix E.

Image-level generation vs. state-level generation. Our work introduces a general data generation method that is agnostic to the specific form of generation. As shown in Figure 6, both image and state generation variants significantly outperform the baselines, while the image-level diffuser generally outperforms the state-level diffuser on the D4RL Locomotion environment. We usually need to synthesize longer and more flexible trajectories in such complicated environments, where the image-level diffuser performs better

| Task Name | TD3+BC | TD3+BC +SynthER | TD3+BC +S4RL | TD3+BC +AtraDiff | IQL | IQL+ SynthER | IQL+ S4RL | IQL+ AtraDiff |
|--------------------|--------|--------------------|-----------------|---------------------|--------------|-----------------|--------------|------------------|
| halfcheetah-random | 11.3 | 12.2 | 11.5 | 12.5 | 15.2 | 17.2 | 15.8 | 17.1 |
| halfcheetah-medium | 48.1 | 49.9 | 48.5 | 52.3 | 48.3 | 49.6 | 48.8 | 53.1 |
| halfcheetah-replay | 44.8 | 45.9 | 45.9 | 46.5 | 43.5 | 46.7 | 46.3 | 49.2 |
| halfcheetah-expert | 90.8 | 87.2 | 91.2 | 93.6 | 94.6 | 93.3 | 94.3 | 95.2 |
| hopper-random | 8.6 | 14.6 | 9.4 | 15.2 | 7.2 | 7.7 | 7.4 | 8.1 |
| hopper-medium | 60.4 | 62.5 | 63.4 | 65.7 | 62.8 | 72.0 | 70.3 | 72.4 |
| hopper-replay | 64.4 | 63.4 | 62.3 | 64.7 | 84.6 | 103.2 | 95.6 | 103.6 |
| hopper-expert | 101.1 | 105.4 | 103.5 | 111.2 | 106.2 | 110.8 | 108.1 | 113.6 |
| walker-random | 0.6 | 2.3 | 3.2 | 2.1 | 4.1 | 4.2 | 4.1 | 4.3 |
| walker-medium | 82.7 | 84.8 | 83.7 | 87.5 | 84.0 | 86.7 | 84.5 | 89.1 |
| walker-replay | 85.6 | 90.5 | 88.3 | 86.3 | 82.6 | 83.3 | 83.1 | 85.4 |
| walker-expert | 110.0 | 110.2 | 106.3 | 111.2 | 111.7 | 111.4 | 111.3 | 111.7 |

Table 1. Normalized return of offline RL on the D4RL Locomotion benchmark. Our AtraDiff outperforms SynthER and S4RL on almost all the tasks and datasets. While primarily intended for offline-to-online scenarios, AtraDiff also demonstrates strong performance in offline data augmentation.

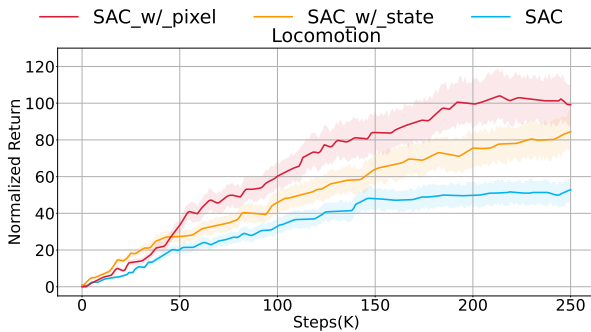


Figure 6. Ablation study on image-level generation and state-level generation. The image-level diffuser outperforms the state-level diffuser in complicated tasks, with noticeable performance gains. compared with simpler diffusion models. Our hypothesis is that image generation can benefit from a pretrained generation model (e.g., Stable Diffusion) while state generation is trained from scratch, though image generation needs additional modules to convert between images and states.

Meanwhile, we conduct an analysis to demonstrate the effectiveness and generalizability of our AtraDiff on pixel-based reinforcement learning methods. To this end, we employ AtraDiff to upsample the dataset from the V-D4RL benchmark (Lu et al., 2022), and use Behavior Cloning (BC) (Torabi et al., 2018) as the baseline to test on the benchmark. The results shown in Table 2 validate that our algorithm is also applicable to the visual reinforcement learning methods, consistently improving their performance.

| Task Name | walker | | | | cheetah | | | |
|-------------|--------|--------|--------|--------|---------|--------|--------|--------|
| Dataset | mixed | medium | medexp | expert | mixed | medium | medexp | expert |
| BC | 16.5 | 40.9 | 47.7 | 91.5 | 25.0 | 51.6 | 57.5 | 67.4 |
| BC+AtraDiff | 17.7 | 42.2 | 50.2 | 93.1 | 25.2 | 55.3 | 68.1 | 85.3 |

Table 2. Normalized return of offline RL on the V-D4RL benchmark. Our AtraDiff consistently improves the performance of pixel-based reinforcement learning methods.

Is online adaptation beneficial for our diffuser? We now examine the effect of online adaptation on performance. We revisit the experiments in Section 5.2 and replace the online adapted diffuser with a fixed one. As shown in Figure 7, we find that the online diffuser significantly outperforms the fixed diffuser in complicated tasks. In tasks of D4RL Locomotion and D4RL AntMaze, the online diffuser achieves comparable results to the fixed diffuser. However, in the task of D4RL Kitchen and two tasks in Meta-World, the online diffuser has fully demonstrated its superiority, which validates that the online adaptation can indeed mitigate the problem of data distribution shift and thus focus on the evaluation task.

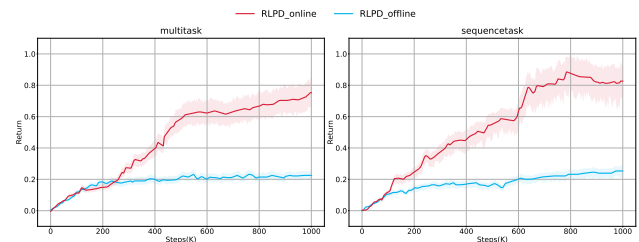


Figure 7. Ablation study on online adaptation of AtraDiff. In simple tasks, we observe that the online diffuser achieves results comparable to the fixed diffuser. However, online adaptation mitigates the problem of data distribution shift and becomes critical in complicated environments.

Effect of different importance indicators over online adaptation. We show that different online adaptation strategies have noticeable impact on performance. Our experiments focus on the indicator used to measure the importance of collected samples together with its associated pick-up strategy for selecting samples according to this importance. We include the Reward indicator and its corresponding pick-up strategy. The result shown in Figure 8 indicates that the TD-error indicator outperforms the Reward indicator.

Effect of different task prompts. We show that different

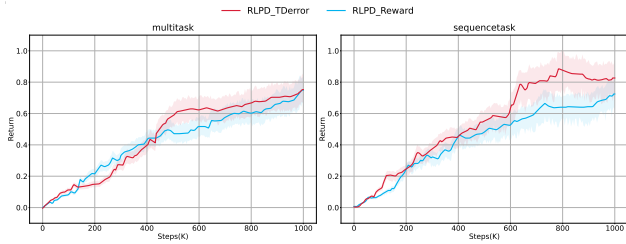


Figure 8. Ablation study on the importance indicator together with its associated pick-up strategy. Different types of indicators lead to varied behavior and performance. While the Reward indicator is in principle more general to RL methods, the indicator based on TD-error achieves better performance in the complicated Meta-World benchmark.

task prompts noticeably affect performance. To evaluate this, we conduct experiments on Meta-World, testing three strategies: language task prompt, one-hot task prompt, and no prompt, where the one-hot prompt simply uses a one-hot vector to represent different tasks. The result shown in Figure 9 demonstrates that the language prompt outperforms the one-hot prompt, and both significantly exceed the performance of the baselines without any prompt.

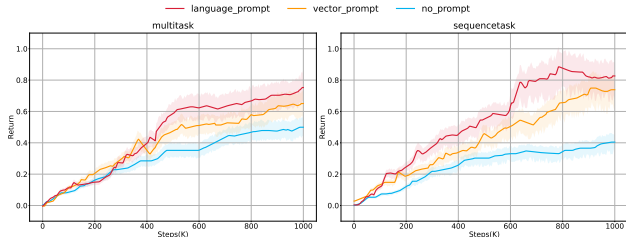


Figure 9. Ablation study on design choices of task prompts. Different types of task prompts lead to varied behavior and performance.

Effect of random dropping strategy. Here we show that the random dropping strategy is very important in the online adaptation process with the Reward indicator. In our online adaptation phase, when using the total reward importance indicator, the importance of any trajectory will never change during the whole training process. Hence, trajectories with high importance might always be used to update the generator, which inspires us to introduce a random dropping strategy. The ablation study conducted on the D4RL Locomotion environment shown in Figure 10 illustrates that the random dropping strategy can significantly improve the performance.

Effect of multi-generator. Now we show that the multi-generator architecture is crucial. We conduct experiments on Meta-World to test the effect of the multiple diffusion model design. We replace the flexible task-length generation control scheme with a fixed length generator of 25, which is the largest length in our setting, and directly apply our pruning strategy after the generation. The result shown in Figure 11 demonstrates that with multiple diffusion models,

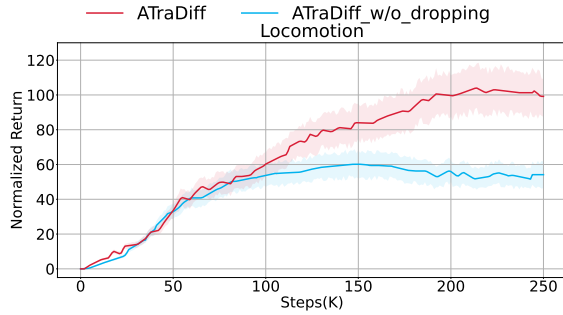


Figure 10. Ablation study on the random dropping strategy. We observe that the random dropping strategy can significantly improve the performance, which validates that different strategies indeed influence the performance.

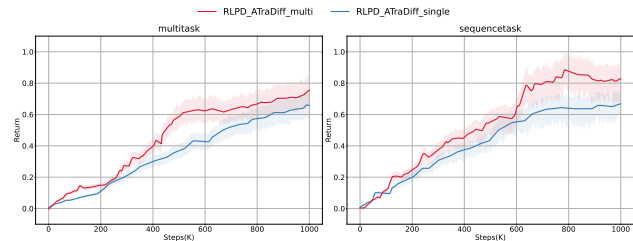


Figure 11. Ablation study on multiple diffusion models. We observe that the performance of ATraDiff with multiple diffusion models significantly outperforms the fixed single diffusion model.

the performance of our method significantly outperforms the fixed single diffusion model.

6. Conclusion

We introduce ATraDiff, a novel diffusion-based approach that synthesizes full trajectories. By training a set of diffusion models that generate trajectories of different lengths and selecting the most suitable model together with a non-parametric pruning algorithm, we obtain a generator that produces trajectories with varied lengths. By applying such a generator to transitions stored in the replay buffer and augmenting the buffer with generated data, ATraDiff can accelerate any online RL algorithm with a replay buffer. In multiple environments, ATraDiff significantly improves existing online, offline, and offline-to-online RL algorithms. We hope that our work is beneficial to the online RL community in addressing the long-standing data efficiency problem.

Limitations and future work. One limitation of ATraDiff is that the training of multiple diffusion models can be computationally intensive (as evaluated in Appendix C.2), and the problem escalates with longer generated trajectories. Thus, an interesting future direction is to learn a single diffuser that directly generates trajectories of varied lengths instead of selecting from a collection of models.

Acknowledgements

This work was supported in part by NSF Grant 2106825, NIFA Award 2020-67021-32799, the Jump ARCHES endowment through the Health Care Engineering Systems Center at Illinois and the OSF Foundation, and the IBM-Illinois Discovery Accelerator Institute. This work used NVIDIA GPUs at NCSA Delta through allocations CIS220014 and CIS230012 from the ACCESS program.

Impact Statement

Our research contributes to decision-making processes by leveraging offline data, aiming to enhance the efficiency of reinforcement learning. While our advancements offer significant benefits in terms of task-solving capabilities, they also raise concerns about potential negative societal impacts. For instance, the deployment of highly efficient autonomous systems in the workforce could lead to job displacement and increased economic inequality. Furthermore, our approach relies on a generative model for synthesizing new data, which introduces concerns regarding the authenticity and reliability of the generated outcomes. The possibility of generating fictitious or misleading data underscores the importance of critically assessing and mitigating potential ethical and societal implications, ensuring that advancements in autonomous decision-making contribute positively to society while minimizing adverse effects.

References

- Ajay, A., Du, Y., Gupta, A., Tenenbaum, J. B., Jaakkola, T. S., and Agrawal, P. Is conditional generative modeling all you need for decision making? In *ICLR*, 2023.
- Ball, P. J., Smith, L., Kostrikov, I., and Levine, S. Efficient online reinforcement learning with offline data. In *ICML*, 2023.
- Black, K., Nakamoto, M., Atreya, P., Walke, H., Finn, C., Kumar, A., and Levine, S. Zero-shot robotic manipulation with pretrained image-editing diffusion models. In *ICLR*, 2024.
- Chen, H., Lu, C., Ying, C., Su, H., and Zhu, J. Offline reinforcement learning via high-fidelity generative behavior modeling. In *ICLR*, 2023.
- Chen, X., Wang, C., Zhou, Z., and Ross, K. W. Randomized ensembled double Q-learning: Learning fast without a model. In *ICLR*, 2021.
- Du, Y., Yang, M., Dai, B., Dai, H., Nachum, O., Tenenbaum, J. B., Schuurmans, D., and Abbeel, P. Learning universal policies via text-guided video generation. In *NeurIPS*, 2023.
- Fu, J., Kumar, A., Nachum, O., Tucker, G., and Levine, S. D4RL: Datasets for deep data-driven reinforcement learning. *arXiv: 2004.07219*, 2020.
- Gong, S., Li, M., Feng, J., Wu, Z., and Kong, L. DiffuSeq: Sequence to sequence text generation with diffusion models. In *ICLR*, 2023.
- Gupta, A., Kumar, V., Lynch, C., Levine, S., and Hausman, K. Relay policy learning: Solving long-horizon tasks via imitation and reinforcement learning. In *CoRL*, 2019.
- Haarnoja, T., Zhou, A., Abbeel, P., and Levine, S. Soft actor-critic: Off-policy maximum entropy deep reinforcement learning with a stochastic actor. *ICML*, 2018.
- Hafner, D., Lillicrap, T. P., Norouzi, M., and Ba, J. Mastering Atari with discrete world models. In *ICLR*, 2021.
- Hansen, N., Lin, Y., Su, H., Wang, X., Kumar, V., and Rajeswaran, A. Modem: Accelerating visual model-based reinforcement learning with demonstrations. In *ICLR*, 2023.
- He, H., Bai, C., Xu, K., Yang, Z., Zhang, W., Wang, D., Zhao, B., and Li, X. Diffusion model is an effective planner and data synthesizer for multi-task reinforcement learning. In *NeurIPS*, 2023.
- Hester, T., Vecerik, M., Pietquin, O., Lanctot, M., Schaul, T., Piot, B., Horgan, D., Quan, J., Sendonaris, A., Osband, I., Dulac-Arnold, G., Agapiou, J., Leibo, J., and Gruslys, A. Deep Q-learning from demonstrations. In *AAAI*, 2018.
- Ho, J., Jain, A., and Abbeel, P. Denoising diffusion probabilistic models. In *NeurIPS*, 2020.
- Janner, M., Du, Y., Tenenbaum, J. B., and Levine, S. Planning with diffusion for flexible behavior synthesis. In *ICML*, 2022.
- Kalashnikov, D., Irpan, A., Pastor, P., Ibarz, J., Herzog, A., Jang, E., Quillen, D., Holly, E., Kalakrishnan, M., Vanhoucke, V., and Levine, S. Scalable deep reinforcement learning for vision-based robotic manipulation. In *CoRL*, 2018.
- Kipf, T., Li, Y., Dai, H., Zambaldi, V. F., Sanchez-Gonzalez, A., Grefenstette, E., Kohli, P., and Battaglia, P. W. Compile: Compositional imitation learning and execution. In *ICML*, 2019.
- Kostrikov, I., Nair, A., and Levine, S. Offline reinforcement learning with implicit Q-learning. In *ICLR*, 2022.
- Kumar, A., Yazdanbakhsh, A., Hashemi, M., Swersky, K., and Levine, S. Data-driven offline optimization for architecting hardware accelerators. In *ICLR*, 2022.

- Laskin, M., Lee, K., Stooke, A., Pinto, L., Abbeel, P., and Srinivas, A. Reinforcement learning with augmented data. In *NeurIPS*, 2020.
- Li, X., Thickstun, J., Gulrajani, I., Liang, P., and Hashimoto, T. B. Diffusion-LM improves controllable text generation. In *NeurIPS*, 2022.
- Lu, C., Ball, P. J., Rudner, T. G. J., Parker-Holder, J., Osborne, M. A., and Teh, Y. W. Challenges and opportunities in offline reinforcement learning from visual observations. *arXiv:2206.04779*, 2022.
- Lu, C., Ball, P. J., Teh, Y. W., and Parker-Holder, J. Synthetic experience replay. In *NeurIPS*, 2023.
- Merel, J., Hasenclever, L., Galashov, A., Ahuja, A., Pham, V., Wayne, G., Teh, Y. W., and Heess, N. Neural probabilistic motor primitives for humanoid control. In *ICLR*, 2019.
- Mirhoseini, A., Goldie, A., Yazgan, M., Jiang, J. W., Songhori, E. M., Wang, S., Lee, Y.-J., Johnson, E., Pathak, O., Nazi, A., Pak, J., Tong, A., Srinivasa, K., Hang, W., Tuncer, E., Le, Q. V., Laudon, J., Ho, R., Carpenter, R., and Dean, J. A graph placement methodology for fast chip design. *Nature*, 594(7862):207–212, 2021.
- Nair, A., McGrew, B., Andrychowicz, M., Zaremba, W., and Abbeel, P. Overcoming exploration in reinforcement learning with demonstrations. In *ICRA*, 2018.
- Nair, A., Gupta, A., Dalal, M., and Levine, S. AWAC: Accelerating online reinforcement learning with offline datasets. *arXiv: 2006.09359*, 2021.
- Pearce, T., Rashid, T., Kanervisto, A., Bignell, D., Sun, M., Georgescu, R., Macua, S. V., Tan, S. Z., Momennejad, I., Hofmann, K., and Devlin, S. Imitating human behaviour with diffusion models. In *ICLR*, 2023.
- Pertsch, K., Lee, Y., and Lim, J. J. Accelerating reinforcement learning with learned skill priors. In *CoRL*, 2020.
- Rombach, R., Blattmann, A., Lorenz, D., Esser, P., and Ommer, B. High-resolution image synthesis with latent diffusion models. In *CVPR*, 2022.
- Schaul, T., Quan, J., Antonoglou, I., and Silver, D. Prioritized experience replay. In *ICLR*, 2016.
- Seo, Y., Hafner, D., Liu, H., Liu, F., James, S., Lee, K., and Abbeel, P. Masked world models for visual control. In *CoRL*, 2022.
- Shirley, P. *Realistic ray tracing*. A K Peters, 2000.
- Siegel, N. Y., Springenberg, J. T., Berkenkamp, F., Abdolmaleki, A., Neunert, M., Lampe, T., Hafner, R., Heess, N., and Riedmiller, M. Keep doing what worked: Behavioral modelling priors for offline reinforcement learning. In *ICLR*, 2020.
- Singh, A., Liu, H., Zhou, G., Yu, A., Rhinehart, N., and Levine, S. Parrot: Data-driven behavioral priors for reinforcement learning. In *ICLR*, 2021.
- Sinha, S., Mandlekar, A., and Garg, A. S4RL: surprisingly simple self-supervision for offline reinforcement learning in robotics. In *CoRL*, 2021.
- Specht, J. M. and Madlener, R. Deep reinforcement learning for the optimized operation of large amounts of distributed renewable energy assets. *Energy and AI*, 11: 100215, 2023.
- Torabi, F., Warnell, G., and Stone, P. Behavioral cloning from observation. In *IJCAI*, 2018.
- Večerík, M., Hester, T., Scholz, J., Wang, F., Pietquin, O., Piot, B., Heess, N., Rothörl, T., Lampe, T., and Riedmiller, M. Leveraging demonstrations for deep reinforcement learning on robotics problems with sparse rewards. *arXiv: 1707.08817*, 2017.
- Wang, S., Jia, D., and Weng, X. Deep reinforcement learning for autonomous driving. *arXiv:1811.11329*, 2019.
- Wang, Z., Hunt, J. J., and Zhou, M. Diffusion policies as an expressive policy class for offline reinforcement learning. In *ICLR*, 2023.
- Whitney, W. F., Agarwal, R., Cho, K., and Gupta, A. Dynamics-aware embeddings. In *ICLR*, 2020.
- Yarats, D., Kostrikov, I., and Fergus, R. Image augmentation is all you need: Regularizing deep reinforcement learning from pixels. In *ICLR*, 2021.
- Yu, T., Quillen, D., He, Z., Julian, R., Hausman, K., Finn, C., and Levine, S. Meta-World: A benchmark and evaluation for multi-task and meta reinforcement learning. In *CoRL*, 2019.
- Zhang, H., Xu, W., and Yu, H. Policy expansion for bridging offline-to-online reinforcement learning. In *ICLR*, 2023.
- Zhao, W., Rao, Y., Liu, Z., Liu, B., Zhou, J., and Lu, J. Unleashing text-to-image diffusion models for visual perception. In *ICCV*, 2023.

A. Algorithm Details

A.1. Pick-up Strategies for Online Adaptation

In our training methodology, we have designed different pick-up strategies for handling different importance indicators, recognizing their unique properties and implications for the learning process.

For the TD-error indicator, a *dynamic* approach is employed due to the variable nature of its importance, which can change as the critic function updates during training. To manage this, a heap structure is used to maintain a buffer of 50,000 samples. This buffer is continuously updated to reflect the current importance of each sample, ensuring that even those with initially low importance are retained for potential future relevance. When it comes time to update the diffuser, a selection of 5,000 high-importance samples is drawn from this buffer, aligning the update process with the most pertinent data at that moment.

In contrast, the strategy for reward importance takes into account its *static* characteristic – the sample importance of such an indicator does not change throughout the training. Here, a smaller buffer of 5,000 samples is employed, updated similarly based on importance. However, to counter the risk of high-importance samples perpetually dominating the buffer, a rotation scheme is implemented. After each update, some samples, particularly the older ones, are dropped. This scheme ensures that each sample contributes to the diffuser update for a limited number of times, thus maintaining a fresh and current dataset for training, reflective of the latest environmental interactions.

These tailored strategies highlight a nuanced understanding of how different indicators behave and affect the learning process, ensuring that both dynamic and static aspects of the training data are optimally utilized for updating the diffuser.

A.2. State-level Trajectory Generation

In the state-level generation, we directly generate trajectories consisting of states, actions and rewards, $\{s_t, a_t, r_t, s_{t+1}, a_{t+1}, r_{t+1} \dots\}$. For the architecture of the diffusion model used in the state-level generation, we directly refer to the architecture used in Lu et al. (2023). Meanwhile, we extend the size of the network used from 24 to 128 to support the increased length of generated trajectories.

A.3. Image Encoder

In the image-level generation, an encoder and a decoder are employed for image rendering and key point detection tasks, respectively. The encoder, based on previous work (Lu et al., 2022; Hansen et al., 2023; Seo et al., 2022), captures observations in an environment where an agent operates. The rendered images, set at a resolution of 84×84 , serve as input of the generation model.

B. Details of Experiment Setup

B.1. D4RL

We consider three different environments from D4RL (Fu et al., 2020). We use the original offline dataset from D4RL (Fu et al., 2020).

AntMaze. This domain steps up the complexity by replacing the 2D ball in Maze2D with an 8-DoF “Ant” quadruped robot, adding a layer of morphological complexity. It is a navigation domain that closely resembles real-world robotic navigation tasks. We follow the design of a sparse 0-1 reward strategy in this environment, activated only upon reaching the goal, to test the stitching challenge under more complex conditions.

Locomotion. Comprising tasks like Hopper, HalfCheetah, and Walker2d, the Locomotion domain is a staple in offline deep RL benchmarks. We use the same datasets in D4RL (Fu et al., 2020) for consistency with previous studies, and also experiment with a variety of datasets to observe the effects of different data qualities.

Kitchen. This environment involves controlling a 9-DoF Franka robot in a kitchen setting, interacting with everyday household items like a microwave, kettle, cabinets, an overhead light, and an oven. Each task aims to achieve a specific goal configuration, like opening the microwave and sliding cabinet door, placing the kettle on the burner, and turning on the overhead light. The Kitchen domain serves as a benchmark for multi-task behavior in a realistic, non-navigation setting. Here, the stitching challenge is amplified due to the complexity of the trajectories through the state space, compelling algorithms to generalize to unseen states rather than rely solely on training trajectories.

| Task Name | Subtasks |
|--------------|---|
| Multitask | evaluation task: Push |
| Sequencetask | Sweep, Sweep Into, Coffee Push, Box Close, Push Wall, Peg Insert Side, Basketball, Soccer |

Table 3. Meta-World task settings. We select the push task as the evaluation task for the multi-task environment. We arrange all the 8 *medium* tasks to form the sequence-task environment.

B.2. Meta-World

The Meta-World benchmark (Yu et al., 2019) is a comprehensive suite designed for evaluating and advancing reinforcement learning and multi-task learning algorithms. It features 50 distinct robotic manipulation tasks, offering a diverse and challenging environment for testing the ability of algorithms to generalize and quickly acquire new skills. Following previous work (Hansen et al., 2023), we select a total of 15 tasks from Meta-World based on their difficulty according to Seo et al. (2022), which categorizes tasks into *easy*, *medium*, *hard*, and *very hard* categories. Same as Hansen et al. (2023), we discard *easy* tasks and select all tasks from the remaining 3 categories. Our approach differs from previous studies (Hansen et al., 2023; Seo et al., 2022) in that we solely utilize proprioceptive state information as input of RL agents, rather than RGB frames or combined state information. This choice allows for easier application to general reinforcement learning methods. Following the previous settings, we use a sparse reward signal that only provides a reward of 1 when the current task is solved and 0 otherwise. For the success criteria, we follow the original setting in Meta-World. Table 3 details our multi-task and sequence-task settings.

Training Dataset. The dataset is acquired by training an RL agent with SAC (Haarnoja et al., 2018) on each single task. For the multi-task setting, the entire dataset is combined by all 14 single tasks. For the sequence task, the entire dataset is combined by all 8 single tasks, without any trajectory change.

C. Additional Experimental Results

This section provides supplementary experimental findings, offering detailed insights and further analysis to deepen understanding of the properties of ATraDiff and its components.

C.1. Detailed Online RL Results

Here we present the detailed online RL results of each environment on D4RL Locomotion with all 4 different offline datasets. Figure 12 shows that our ATraDiff is comparable to or better than the original RL baseline methods with low-quality data (such as random data), and the performance gap between our ATraDiff and the baselines becomes much more pronounced with medium/high-quality data (such as medium-expert data).

C.2. Training Time

The experiments are conducted on a single NVIDIA RTX 4090TI GPU. The training time of ATraDiff is listed in Table 4.

| | Walker2D | Hopper | Halfcheetah |
|-----------------------------|----------|--------|-------------|
| SAC (Haarnoja et al., 2018) | 6.5h | 7h | 7h |
| SAC with ATraDiff | 15h | 17h | 16.5h |
| RDEQ (Chen et al., 2021) | 6h | 6.5h | 6.5h |
| RDEQ with ATraDiff | 14.5h | 16.5h | 16h |

Table 4. Time cost (hours) of training SAC and RDEQ with and without ATraDiff.

C.3. Comprehensive Analysis and Further Comparison of ATraDiff and SynthER

ATraDiff differs significantly from SynthER (Lu et al., 2023) in various crucial aspects, particularly in the context of the online learning environment. These aspects collectively contribute to our substantial improvements over SynthER. Below, we summarize several key differences.

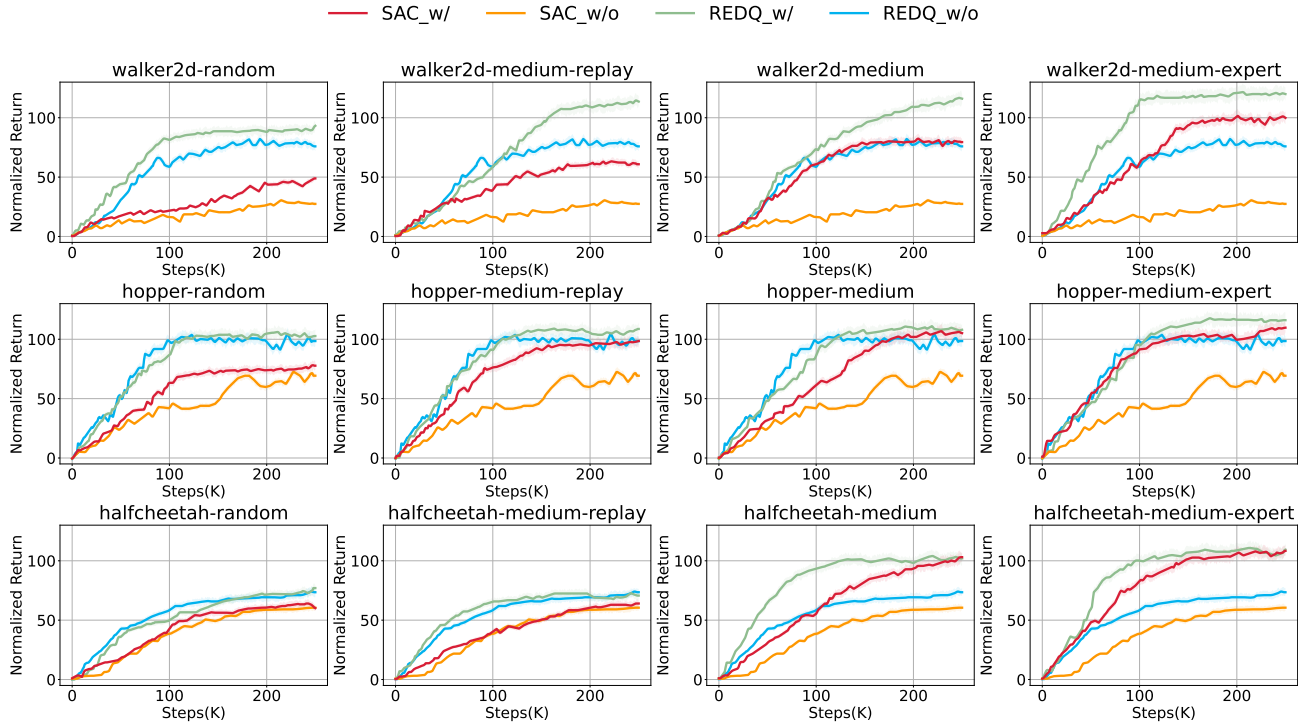


Figure 12. Learning curves of online RL on the D4RL Locomotion benchmark. ATraDiff (denoted as ‘w/’) is comparable to or better than the original RL baseline methods with low-quality data, and the performance gap between ATraDiff and the baselines becomes much more pronounced with medium/high-quality data.

- ATraDiff can perform both image and state generation, with our findings indicating a superior performance of image generation within our framework. This enhancement is likely attributable to the more effective utilization of the pretrained generative model in image generation, as opposed to SynthER’s state-only generation approach.
- Moreover, ATraDiff is designed to synthesize entire trajectories rather than generating individual transitions as in SynthER. We posit that this capability to produce full trajectories yields a richer, more informative dataset for the learning algorithm than isolated transitions.
- In the realm of online training, ATraDiff uniquely generates these trajectories based on the specific current state and task, thereby optimizing the relevance and quality of the generated data for immediate online learning applications.
- In addition to these features, during the online adaptation phase, ATraDiff employs importance sampling strategies to selectively leverage data collected online, prioritizing information that is most beneficial for the online adaptation.

To substantiate the advantages of ATraDiff, we conduct an additional ablation study that systematically evaluates the incremental contributions of its components mentioned above. The study is structured as follows: initially, compared with SynthER, ATraDiff is applied to generate pixel-level single transitions without auxiliary mechanisms, denoted as “_transition.” Subsequently, we evaluate the generation of pixel-level trajectories, still devoid of supplementary techniques, denoted as “_trajectory.” Next, we assessed ATraDiff’s capability to produce pixel-level trajectories informed by the current state, albeit without implementing importance sampling, denoted as “_condition.” Lastly, we evaluate the full ATraDiff, denoted as “_ATraDiff.” The results from this experiment, as presented in Table 5, demonstrate ATraDiff’s progressive improvement, affirming that each technique’s integration significantly boosts the model’s effectiveness, particularly under online training conditions. These findings underscore ATraDiff’s novel, sophisticated methodology in enhancing learning and adaptation in dynamic environments, and explain why ATraDiff notably outperforms SynthER.

| Task Name | SynthER | RLPD_transition | RLPD_trajectory | RLPD_condition | RLPD_ATraDiff |
|--------------|---------|-----------------|-----------------|----------------|---------------|
| Locomotion | 94.6 | 93.5 | 97.1 | 101.3 | 102.3 |
| AntMaze | 97.3 | 97.2 | 97.6 | 98.2 | 98.7 |
| Multitask | 0.57 | 0.60 | 0.72 | 0.75 | 0.77 |
| Sequencetask | 0.62 | 0.64 | 0.71 | 0.79 | 0.81 |

Table 5. Full comparison between ATraDiff and SynthER on both D4RL (normalized return) and Meta-World (return) benchmarks. ATraDiff notably outperforms SynthER, with each of our proposed components contributing to the improvement.

D. Additional Related Work: Discussions on World Models in RL

As an emerging research direction, we recognize the significant potential of world models in decision-making domains. However, we would like to clarify that our work aims to demonstrate a specific application of world models within the RL framework, which is novel, under-explored, and effective, but we do not claim that our method represents the best way of exploiting world models in RL. An evaluation of the optimal strategies is beyond the scope of this paper, and we leave it as interesting future work. We also believe that the optimal approach will likely vary depending on the application and task at hand.

Distinct from studies that create comprehensive decision-making models capable of autonomously completing tasks (e.g., SUSIE (Black et al., 2024) and Dreamerv2 (Hafner et al., 2021)), our work focuses on developing a *versatile auxiliary* method designed to enhance existing RL algorithms. Our contribution is not a standalone task-solving mechanism; rather, it is a plug-in approach intended to integrate seamlessly with any RL algorithm that employs a replay buffer. This distinction underscores the innovative aspect of our work: offering a method that broadens the applicability and efficiency of world models as supportive tools in the RL landscape, thereby facilitating their adoption and utility in diverse RL contexts and applications.

E. Visualizations

In Figure 13, we show some representative visualizations of our generated image trajectories. We present a variety of images generated under different conditions, including varying initial states and a range of tasks. The labels in the left of the figures represent the task. The results demonstrate the robustness and effectiveness of our image generation method, consistently performing well across diverse scenarios and producing high-quality and temporally coherent image trajectories.

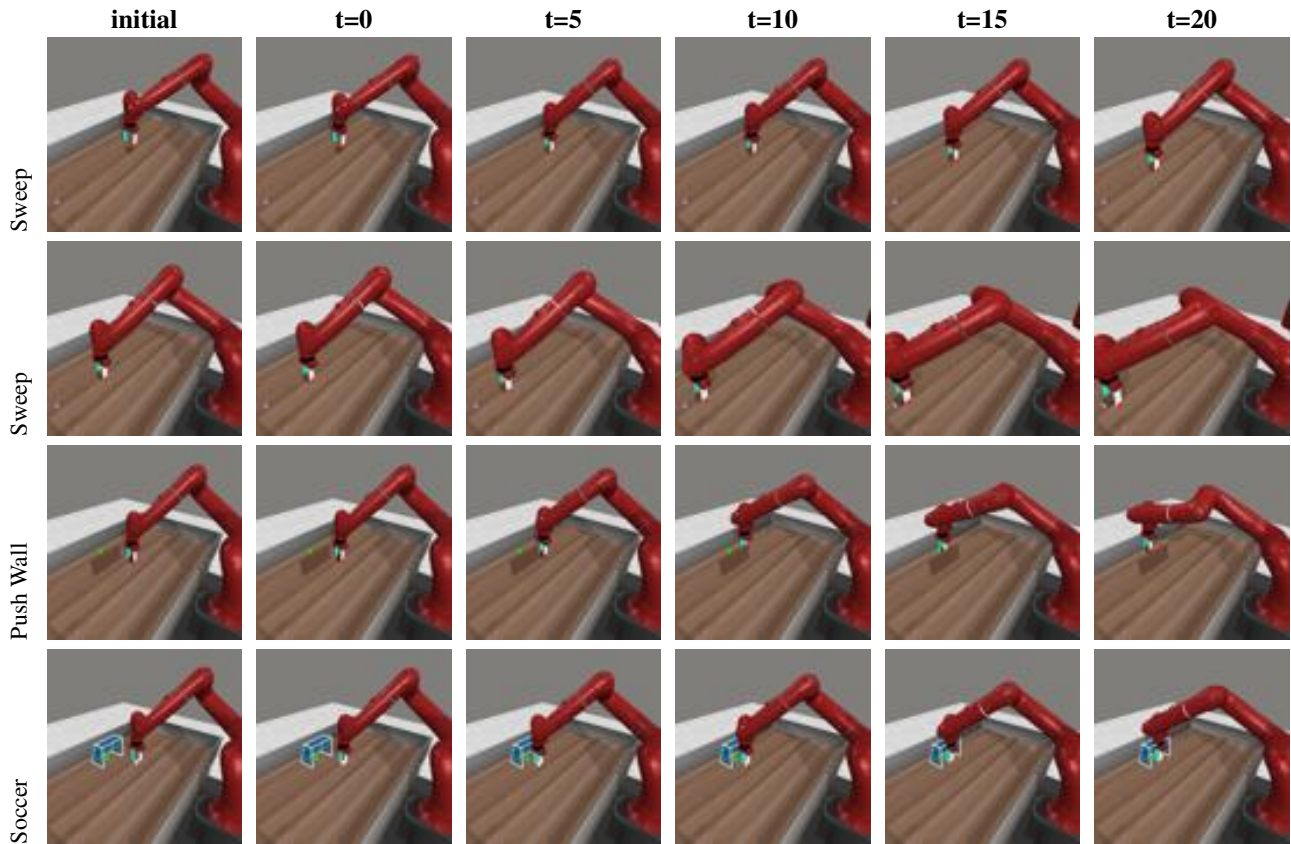


Figure 13. Representative visualizations of our generated image trajectories. Each row contains one generation, the initial image represents the state received by ATraDiff, and the following images represent the generated results in different time-steps.